Angewandte Chemie
Eine Zeitschrift der Gesellschaft Deutscher Chemiker

Supporting Information

An All-Solid-State Fiber-Shaped Aluminum–Air Battery with Flexibility, Stretchability, and High Electrochemical Performance

Yifan Xu[+], *Yang Zhao*[+], *Jing Ren, Ye Zhang, and Huisheng Peng**

anie_201601804_sm_miscellaneous_information.pdf

Supporting Information

Experimental Section

The structures were characterized by scanning electron microscopy (SEM, Hitachi FE-SEM S-4800), transmission electron microscopy (TEM, JEOL JEM-2100F) and optical microscopy (Olympus BX51). The photographs were taken by a camera (Nikon, J1). The fiber-shaped Al-air battery performances were measured at an Arbin electrochemical station (MSTAT-5 V/10 mA/16Ch). The alternating current (AC) impedance spectra of the hydrogel electrolyte, polarization curves and discharging performances of the Al-air battery under bending and stretching were measured through an electrochemical workstation (CHI 660D). All electrochemical measurements were conducted in ambient atmosphere at room temperature (~25°C). The Ag load on the CNT sheet air cathode was calculated on the basis of the surface area of the CNT sheets cross-stacked on the Teflon plate. The mass of the coated Ag nanoparticles was weighed by a micro-balance (Mettler Toledo MX5). The current densities of the cyclic voltammograms of CNT/Ag catalyst were calculated from the mass of the CNT/Ag. The current and power densities were calculated from the surface area of the CNT sheet air cathode. The specific capacities and the energy density of the fiber-shaped Al-air batteries were normalized to the mass of the consumed Al. The power density of the Al-air battery was calculated from the volume of the whole device. The commercial light emission diode watch is typically powered by a lithium cell (CR1220).

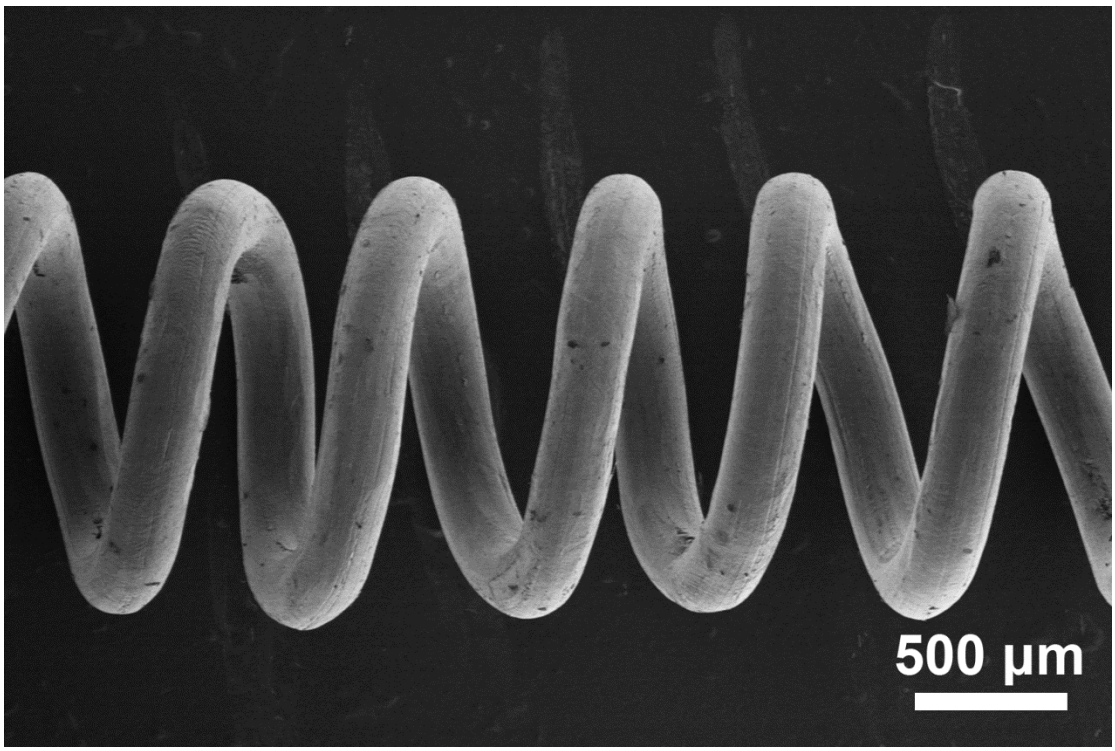

Figure S1. SEM image of an aluminum spring.

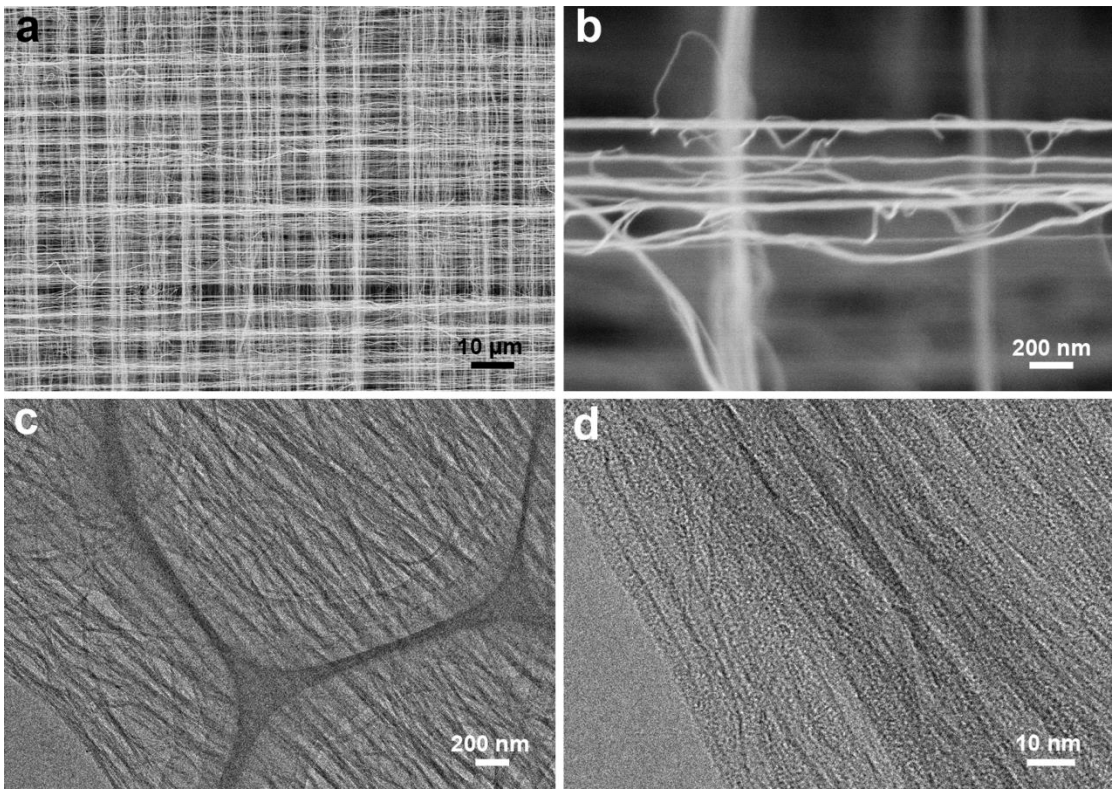

Figure S2. a) and **b**) SEM images of cross-stacked CNT sheets without Ag coating at low and high magnifications, respectively. **c**) and **d**) TEM images of cross-stacked CNT sheets without Ag coating at low and high magnifications, respectively.

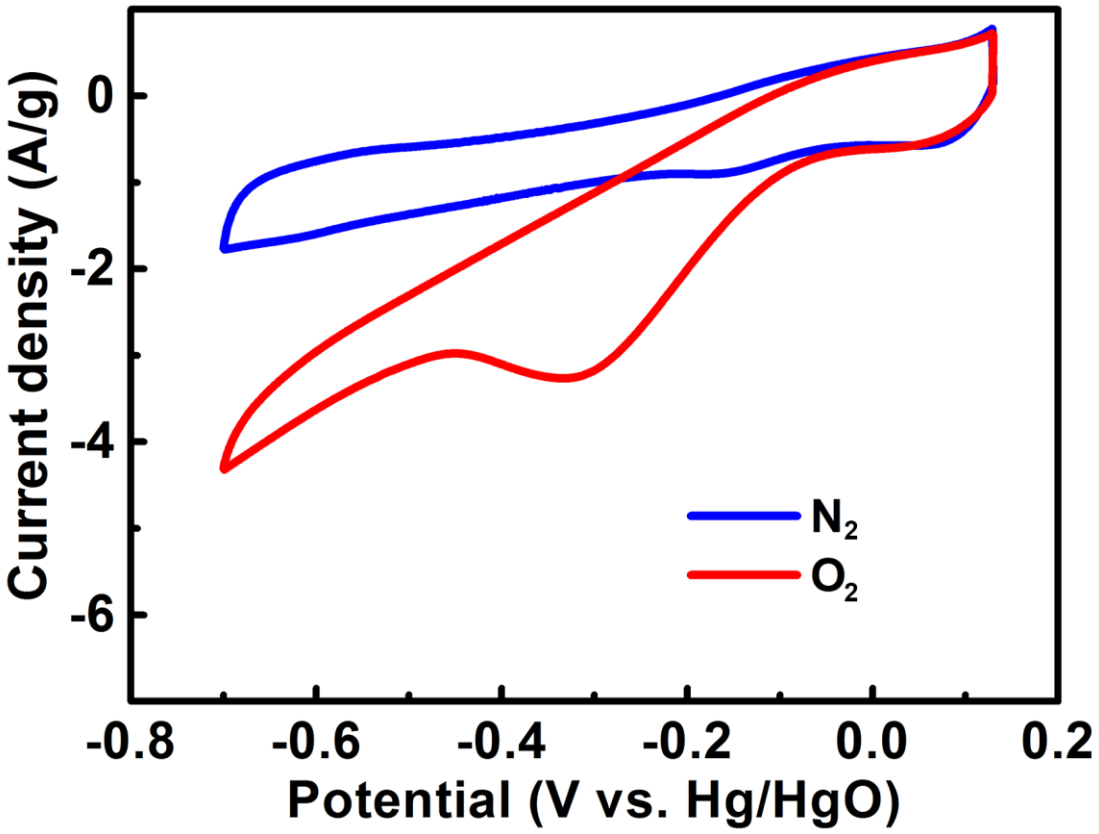

Figure S3. Cyclic voltammograms of CNT/Ag catalyst with Ag load of 45.5 μg/cm^2 in N_2 and O_2 saturated 0.1 M KOH.

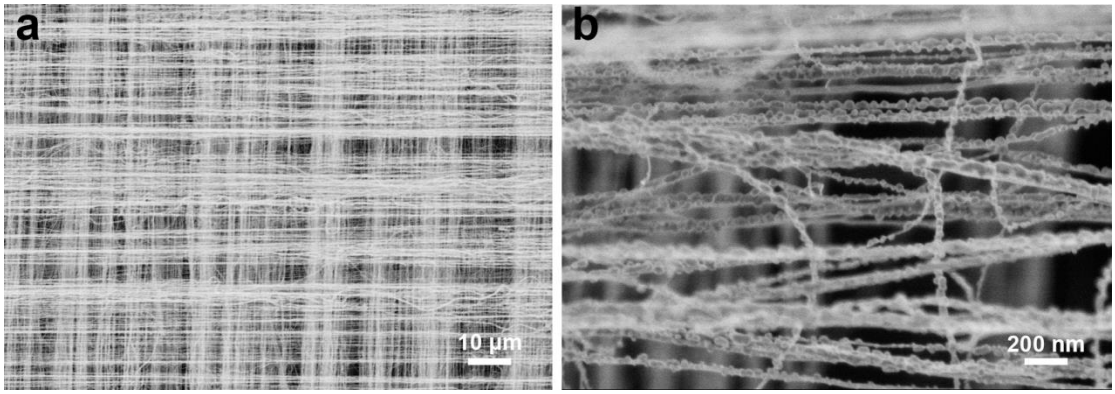

Figure S4. SEM images of cross-stacked CNT sheets with Ag load of 23.3 μg/cm^2 at low (**a**) and high (**b**) magnifications.

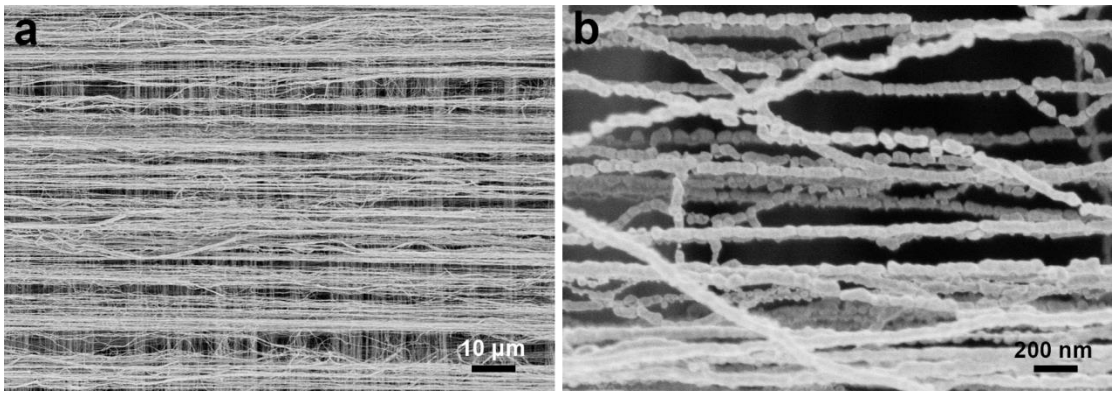

Figure S5. SEM images of cross-stacked CNT sheets with Ag load of 66.9 µg/cm^2 at low (**a**) and high (**b**) magnifications.

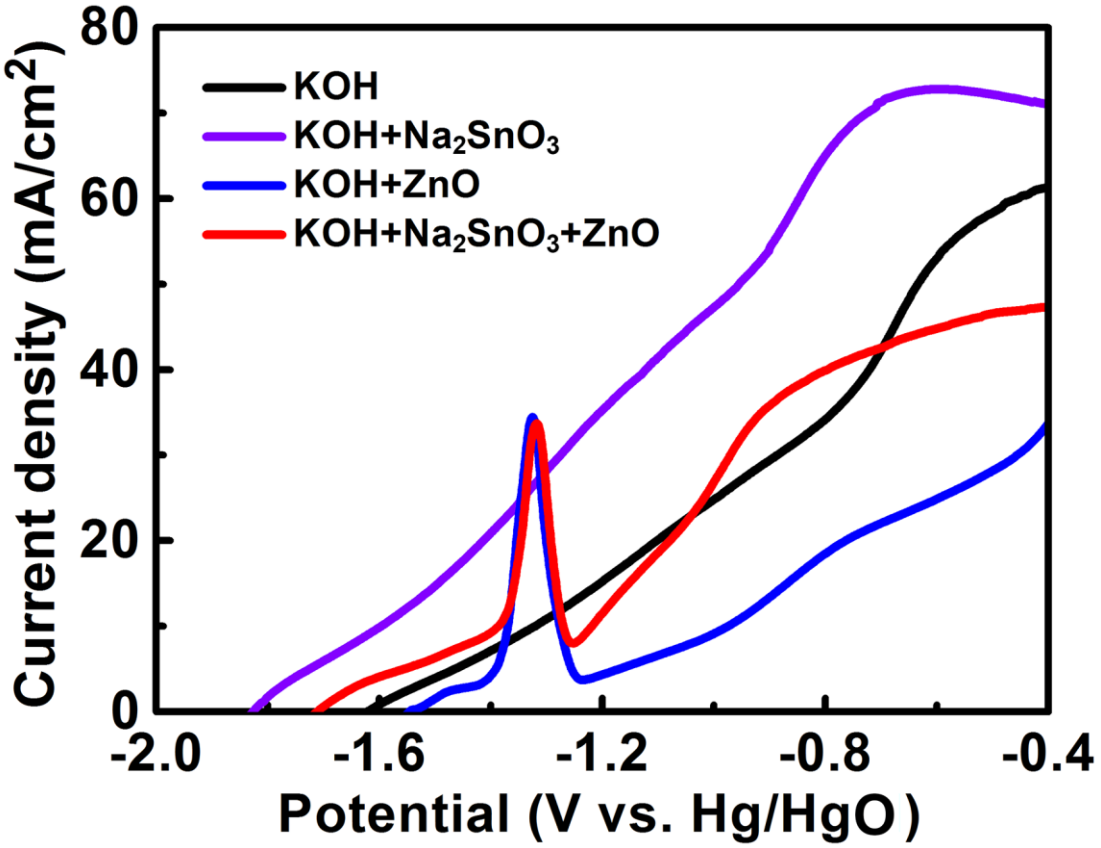

Figure S6. Effect of electrolyte additives on the anode polarization of aluminum (99.999%) in the hydrogel electrolyte (scan rate of 5 mV/s). Counter electrode: platinum electrode. Here the used amount of KOH and additive in the electrolyte remained the same.

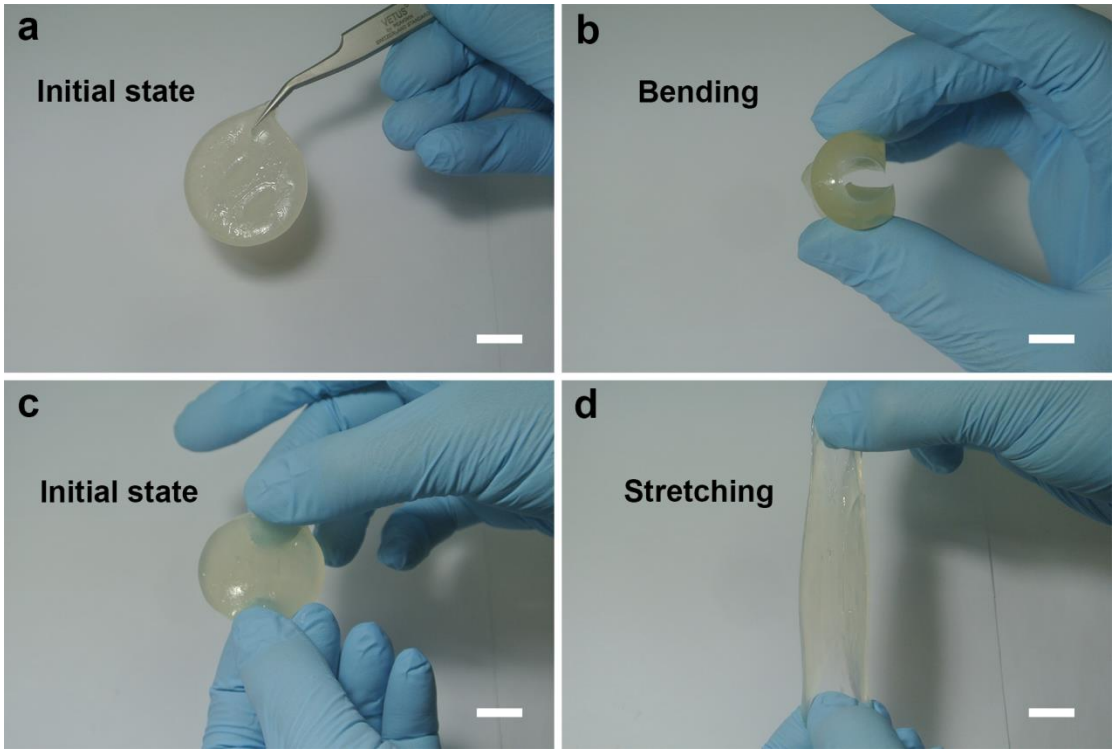

Figure S7. a) and **b**) Photographs of the cross-linked hydrogel electrolyte before and after bending, respectively. **c**) and **d**) Photographs of the cross-linked hydrogel electrolyte before and after stretching, respectively. Scale bar: 1 cm.

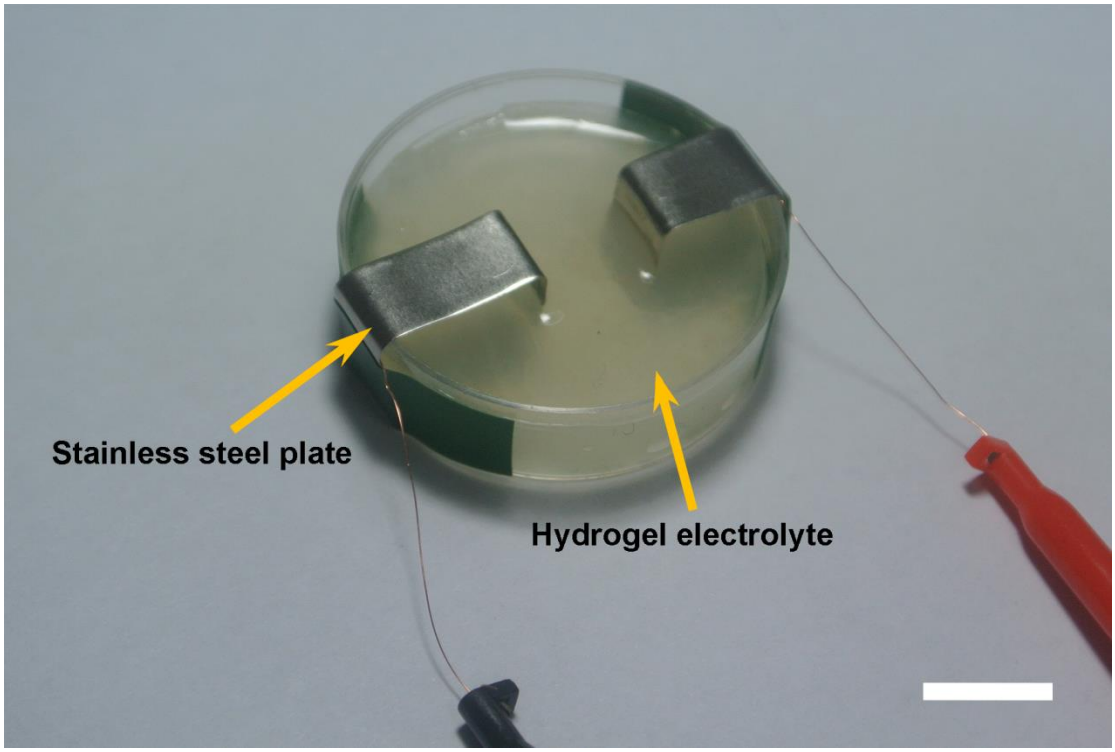

Figure S8. Photograph of measuring the ionic conductivity of hydrogel electrolyte. Scale bar: 1 cm.

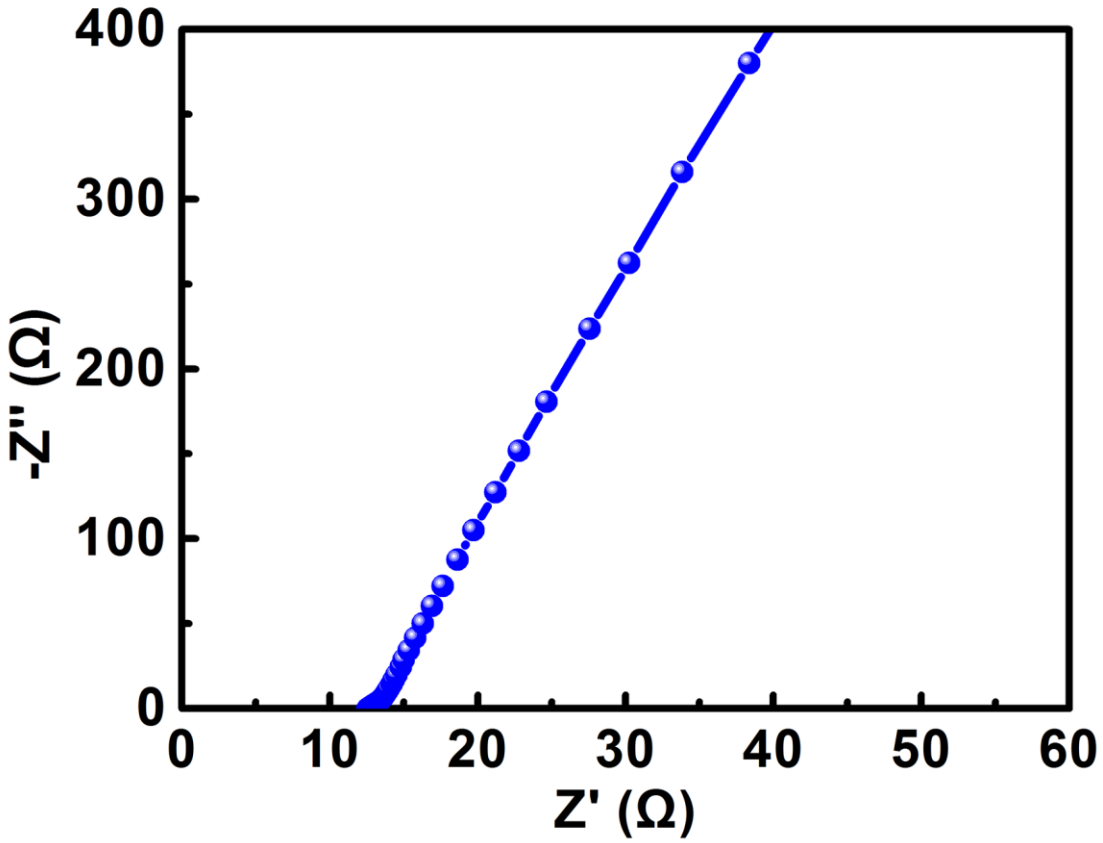

Figure S9. Alternating current impedance spectra of the hydrogel electrolyte at the frequency range from 100 kHz to 0.01 Hz.

The ionic conductivity was calculated by the equation of $\sigma = l/(A \times R)$, where σ represents the ionic conductivity, and l, A and R are the thickness, the area, and the resistance of hydrogel electrolyte between the two stainless plates, respectively. The resistance of the hydrogel electrolyte from the alternating current impedance spectra was 12.5 Ω, and the thickness and area of the electrolyte were 1 cm and 0.45 cm^2, respectively. The conductivity of the hydrogel electrolyte was 0.18 S/cm.

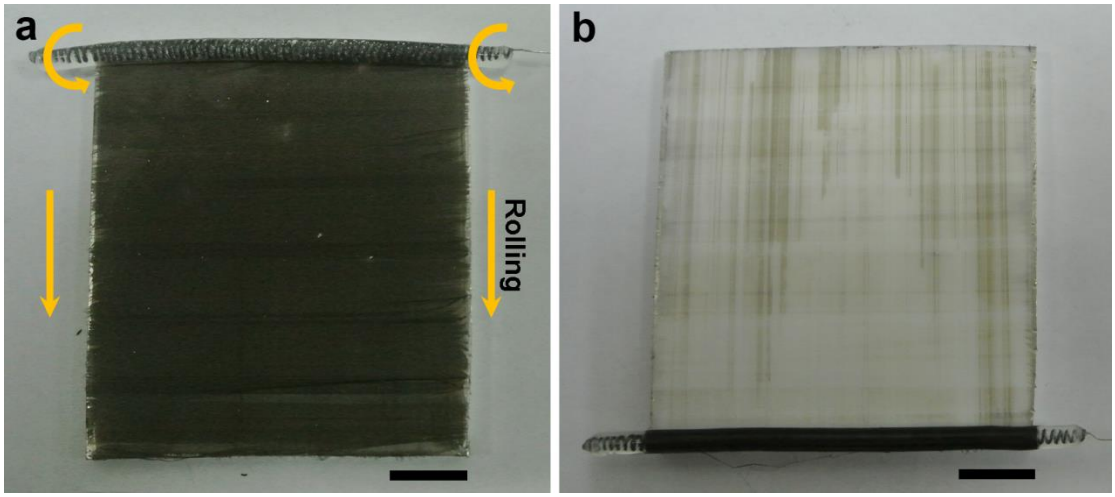

Figure S10. Photographs of wrapping the modified Al spring with the cross-stacked aligned CNT/Ag sheets as air cathode to prepare the fiber-shaped Al-air battery. **a**) and **b**) Before and after rolling, respectively. Scale bar: 1 cm.

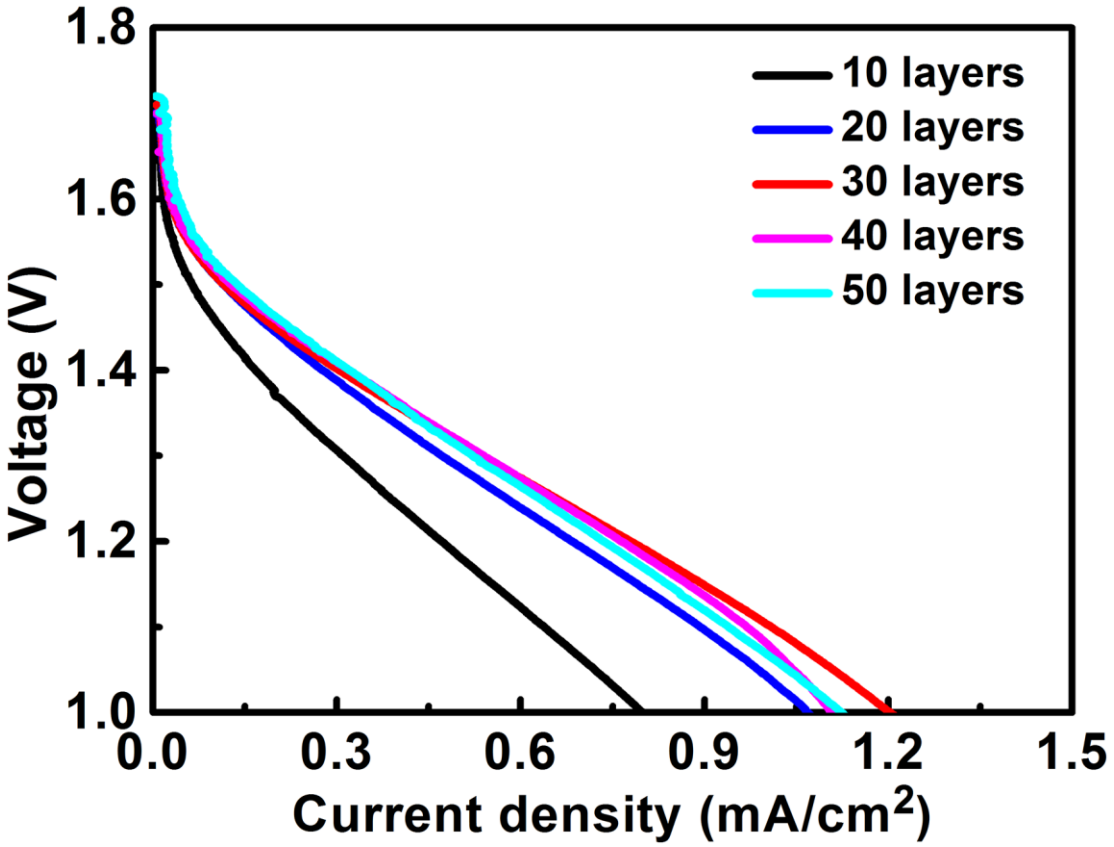

Figure S11. Polarization curves of the fiber-shaped Al-air batteries with increasing layer numbers of CNT sheets (scan rate of 2 mV/s). The loading content of Ag nanoparticles was 45.5 μg/cm^2.

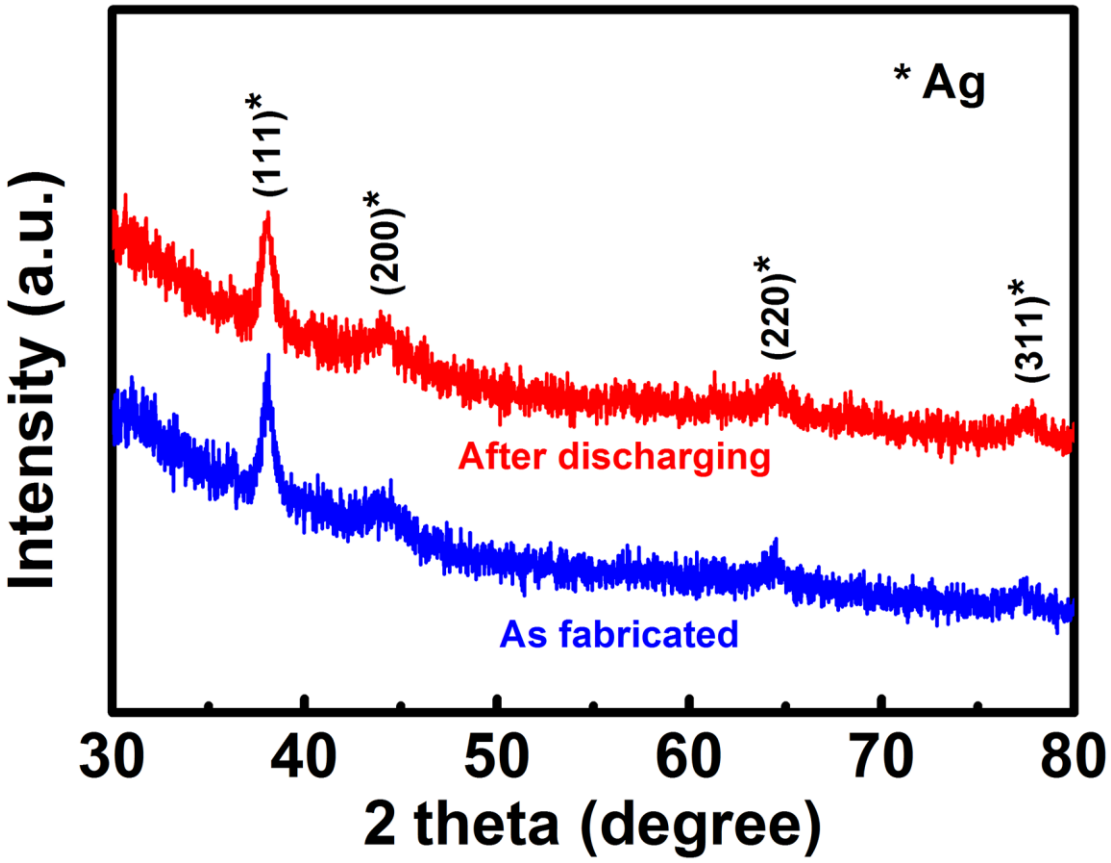

Figure S12. X-ray diffraction patterns of the CNT/Ag sheet air cathode before and after discharging.

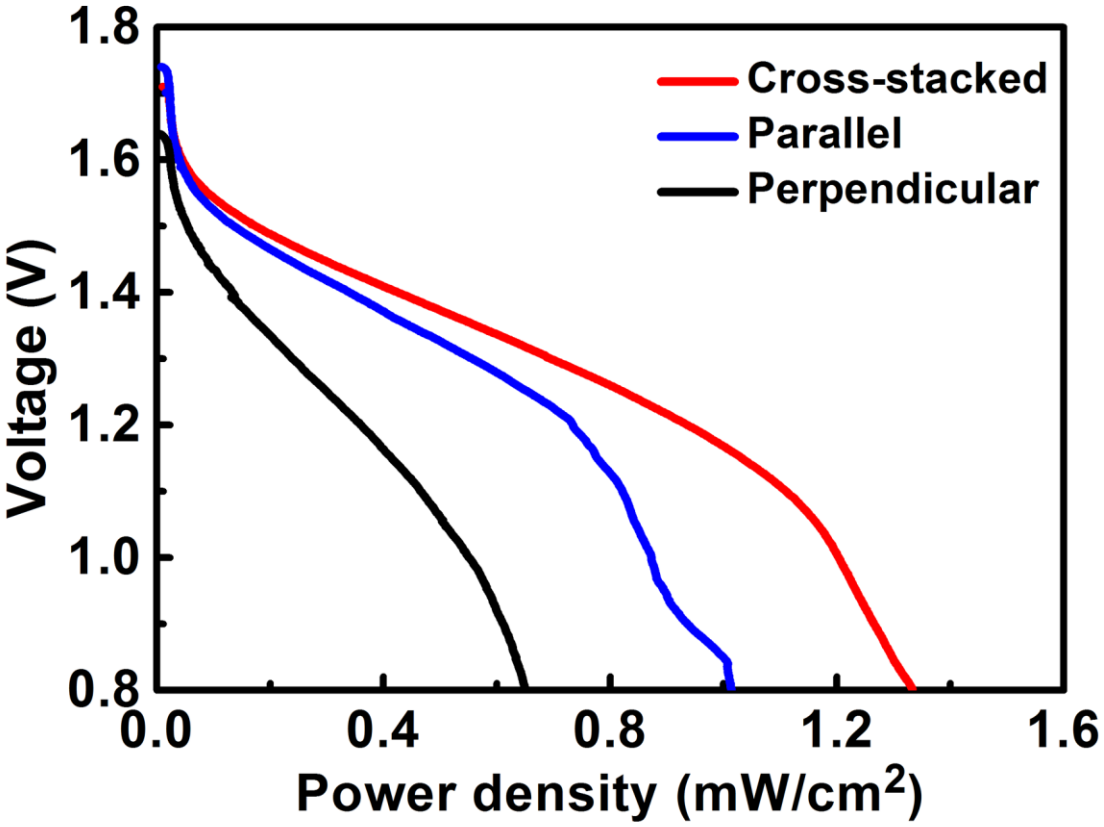

Figure S13. Power density curves of the fiber-shaped Al-air batteries using CNT/Ag sheet air cathodes where CNTs were arranged in a cross-stacked pattern or were parallel or perpendicular to the length direction of the battery fiber.

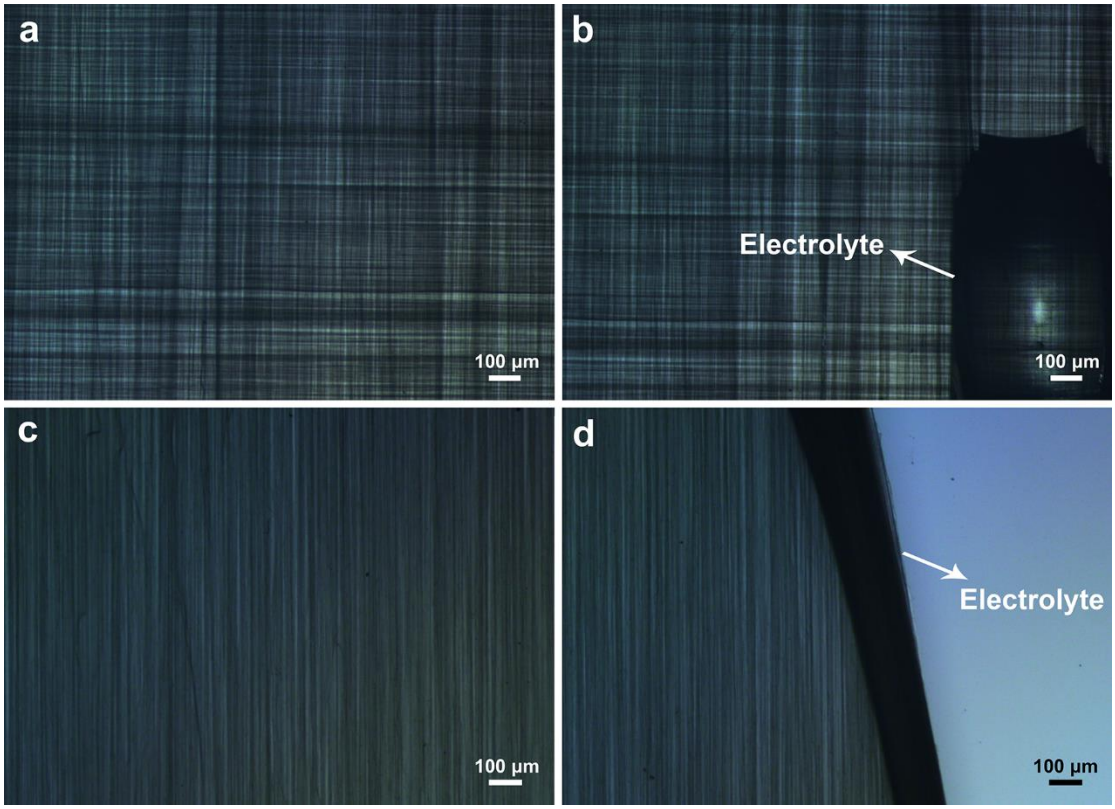

Figure S14. a) and **b**) Optical images of cross-stacked CNT sheets before and after contact with the electrolyte, respectively. **c**) and **d**) Optical images of parallel CNT sheets (the aligned CNTs were stacked along the aligned direction) before and after contact with the electrolyte, respectively.

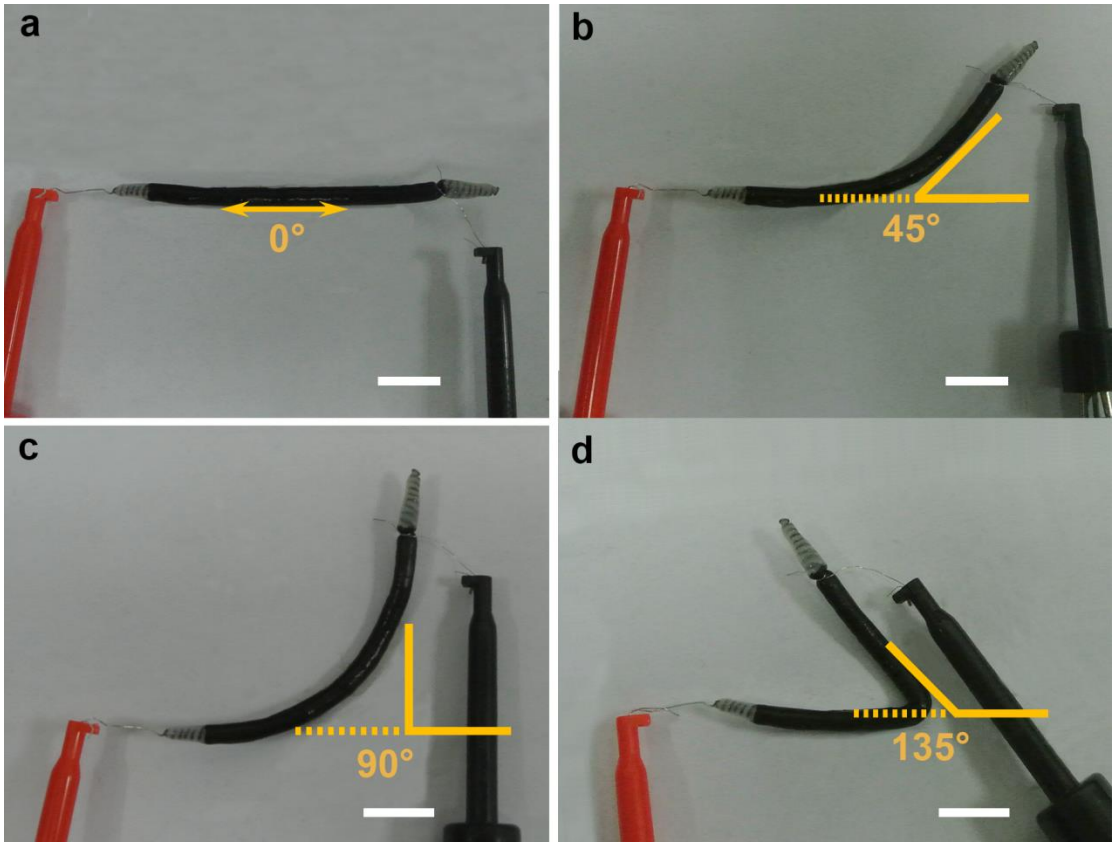

Figure S15. Photographs of an Al-air battery before (**a**) and after bending to 45° (**b**), 90° (**c**) and 135° (**d**). Scale bar: 1cm.

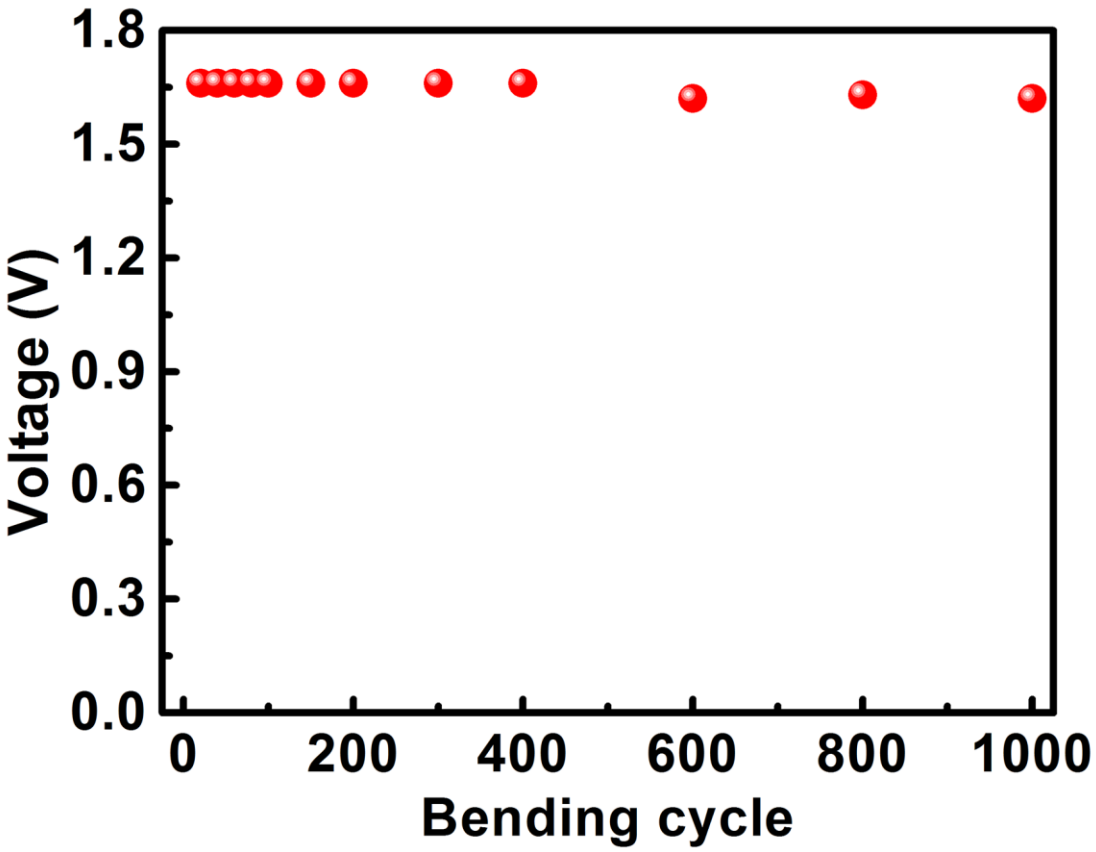

Figure S16. Dependence of open-circuit voltage on bending cycle at a bending angle of approximately 135°.

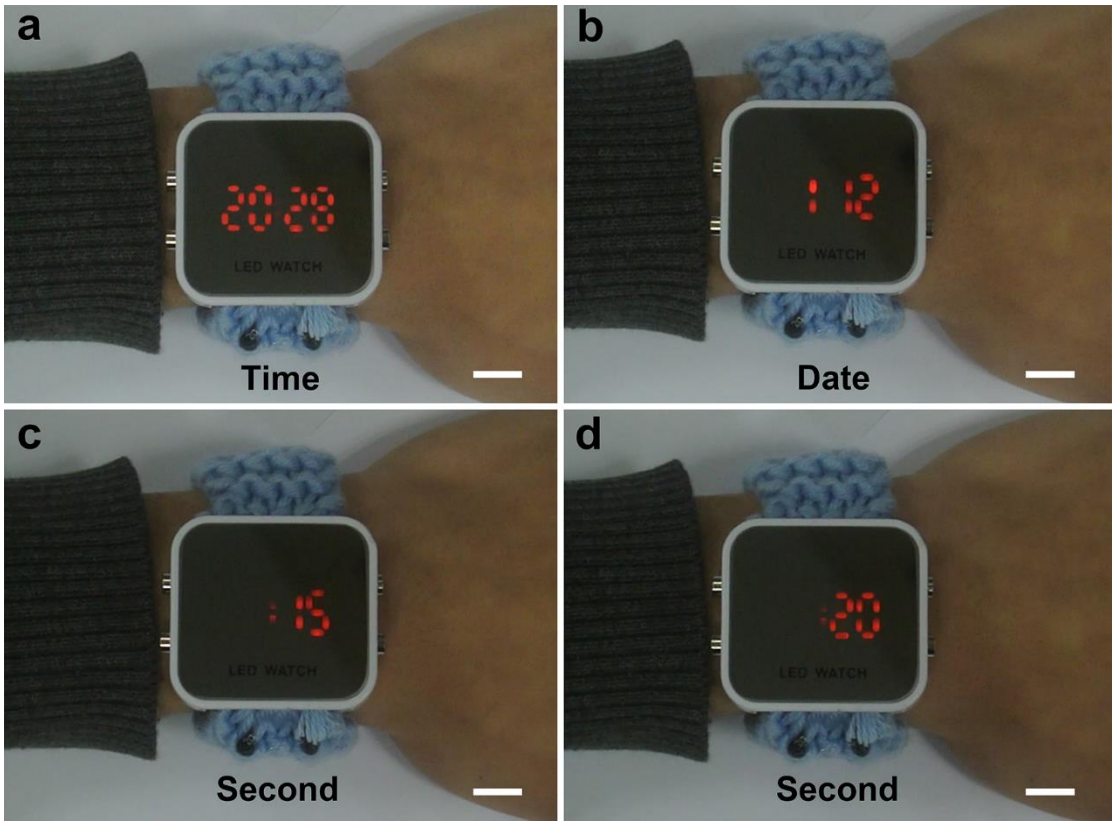

Figure S17. Photographs of a commercial light emission diode (LED) watch powered by two fiber-shaped Al-air battery woven into a fabric and connected in series. The watch showed time (**a**), date (**b**) and second (**c** and **d**). Scale bar: 1 cm.